Radiation Physics and Chemistry 108 (2015) 65–73

Contents lists available at ScienceDirect

Radiation Physics and Chemistry

journal homepage: www.elsevier.com/locate/radphyschem

The influence of defect levels on the dose rate dependence of synthetic diamond detectors of various types on exposures to high-energy radiotherapy beams

N. Ade, T.L. Nam *

School of Physics, Radiation and Health Physics Unit and DST-NRF Centre of Excellence in Strong Materials, University of the Witwatersrand, Private Bag 3, Wits 2050, Johannesburg, South Africa

HIGHLIGHTS

- Dose rate linearity index Δ was evaluated for various diamonds using two beam types.
- Only Δ values of a HPHT diamond were independent of both beam energy and type.
- Presence of C–H and N3 defect-centres linked to variation of Δ with beam energy.
- Δ Values of diamonds with low defect levels show $\leq 2.2\%$ change with bias voltage.

ARTICLE INFO

Article history:
Received 5 June 2014
Received in revised form
6 November 2014
Accepted 21 November 2014
Available online 24 November 2014

Keywords:
Diamond detectors
Photons
Electrons
Dose rate dependence
Defects

ABSTRACT

The linear response of a radiation dosimeter with absorbed dose rate is a principal requirement in radiotherapy. Fowler's model for electrical conductivity, σ of a solid-state detector and absorbed dose rate, D_r is of the form $\sigma \propto D_r^{\Delta}$ where Δ is the linearity index that can take on a range of values around unity. Utilising synthetic diamond detectors of various types as sensors, this study investigates the influence of defect levels on the Δ values of the sensors and the dependence of Δ on bias voltage, beam energy and type in the dosimetry of high-energy photon and electron therapy beams. One main objective of the study was to establish whether for a given diamond detector, Δ could be determined only once for any given beam energy and then used for other beam energies of clinical interest. In order to attain the ICRU overall $\pm 5\%$ uncertainty of absorbed dose delivery in radiotherapy, $\pm 2\%$ accuracy was considered. The study was conducted on one HPHT and eight CVD synthesised diamonds of optical grade (OG) and detector grade (DG) qualities using 6 and 15 MV photon, and 7 and 12 MeV electron energies. Values of Δ ranging from 0.79–1.03 to 0.85–0.96 were obtained for the electron and photon beams, respectively for all the diamond sensors at 1 kV/cm. The Δ values were found to change with various defect levels present within the crystals as characterised by Raman spectroscopy, ESR, FTIR spectroscopy and TL emission, and it was observed that the Δ values of crystals with high defect levels varied strongly with bias voltage. Whereas the Δ values of the HPHT diamond were found not vary with the electron and photon energies, only those of three CVD samples of a given class showed a variation within 2% between the two energies of each beam type. However, for all the crystals tested Δ showed a maximum variation of 3.4% between the photon energies unlike the electron energies where a very strong variation ($> 5\%$) was observed for three OG CVD crystals. The results of this study have suggested that differences in crystal quality due to the presence of defects could cause Δ to vary with bias voltage, beam energy and type.

1. Introduction

The linear response of a radiation detector with absorbed dose rate on exposure to radiotherapy beams is necessary (Marczewska et al., 2007), given the required performance of the detector in electron depth–dose distribution measurements where high dose gradients are generally present and bremsstrahlung contamination exist (van der Merwe and Keddy, 1999). Like silicon diodes, diamond detectors are well-known to show dose rate dependence (Planskoy, 1980; Laub et al., 1997, 1999; Buttar et al., 2000; Cirrone et al., 2006; Schirru et al., 2008) in accordance with Fowler (1966) model of induced conductivity in insulating materials. The relationship between electrical conductivity, σ of a solid-state detector and absorbed dose rate, D_r is of the form (Fowler, 1966)

* Corresponding author.
E-mail address: Tom.Nam@wits.ac.za (T.L. Nam).

http://dx.doi.org/10.1016/j.radphyschem.2014.11.016
0969-806X/

Table 1
Synthetic diamond detectors and their characteristics.

Diamond crystals	Dimensions (mm^3)	Dark current (nA) at 1 kV/cm	Raman characteristics			TL response (a.u)	ESR [N_s] (± 2 ppm/ppb)	FTIR abs-integrated area under peaks (a.u)				Δ Values (± 0.02) at 1 kV/cm for			
			FWHM (cm^{-1})	Shift $\Delta\upsilon$ (cm^{-1})	Stress (GPa)[a]			[C–H]	[A/B]	[N3]	[A]	Electron beams		Photon beams	
												7 MeV	12 MeV	6 MV	15 MV
HPHT	$8.0 \times 6.4 \times 1.0$	0.01	2.27 ± 0.04	0.02 ± 0.01	-0.01	2.2	130 ppm	4	3	34	–	0.95	0.95	0.96	0.96
OGA1	$5.0 \times 5.0 \times 1.0$	0.07	2.56 ± 0.09	0.01 ± 0.04	0.00	13.8	43 ppm	20	26	60	–	0.94	0.86	0.94	0.91
OGA2	$5.0 \times 5.0 \times 1.0$	0.07	2.42 ± 0.09	0.02 ± 0.04	-0.01	11.4	71 ppm	14	31	55	–	0.92	0.84	0.88	0.85
DGA1	$5.0 \times 5.0 \times 1.0$	0.35	2.60 ± 0.09	0.08 ± 0.14	-0.03	45.0	3.5 ppm	65	50	143	2	0.91	0.87	0.91	0.89
DGA2	$5.0 \times 5.0 \times 1.0$	0.14	2.55 ± 0.09	0.07 ± 0.12	-0.02	19.1	5 ppm	36	22	78	1	0.82	0.79	0.87	0.85
DGA	$10.0 \times 10.0 \times 0.5$	0.14	2.34 ± 0.08	0.08 ± 0.10	-0.03	0.74	20 ppb	12	27	19	–	1.02	1.01	0.91	0.92
DGB1	$10.0 \times 10.0 \times 0.5$	0.07	2.37 ± 0.11	0.10 ± 0.14	-0.03	0.82	10 ppb	14	37	39	–	1.01	0.99	0.96	0.95
OGA	$10.0 \times 10.0 \times 1.0$	0.20	2.42 ± 0.11	0.03 ± 0.09	-0.01	1.24	50 ppb	6	11	7	1	1.01	0.96	0.91	0.89
OGD	$10.0 \times 10.0 \times 1.0$	0.25	2.46 ± 0.25	0.06 ± 0.17	-0.02	1.76	46 ppb	15	12	19	3	1.03	1.01	0.94	0.95

[a] The residual stress $S = \Delta\upsilon/\alpha = (\upsilon_m - \upsilon_o)/\alpha$, where υ_o is unstressed peak = 1332.74 cm^{-1}, υ_m is the measured diamond Raman peak and $\alpha = 2.88$ cm^{-1} GPa^{-1}.

$$\sigma \propto D_r^{\Delta} \quad (1)$$

where Δ is the linearity index that can take on a range of values around unity (usually $0.5 \leq \Delta \leq 1.0$) depending on the material characteristics. The detector will therefore not be dependent on dose rate if Δ is unity.

The parameter Δ is an important property of diamond detectors since it determines both the linearity of a given diamond detector and also gives an indication of crystal quality as its value is known to be influenced by the presence or absence of crystal imperfections. Additionally, the change in conductivity with dose rate has been noted to be significant (Hoban et al., 1994). Because of the influential role of Δ in radiation dosimetry, we are therefore motivated to study the dose rate dependence of synthetic diamond detectors of various types in the dosimetry of conventional radiotherapy beams. The aim was to investigate in particular the influence of defect levels on the Δ values of the diamond detectors and the dependence of Δ on bias voltage, beam energy and type in the dosimetry of high-energy photon and electron therapy beams. One main objective was to establish whether for a given diamond detector, Δ could be determined only once for any given beam energy and then used for other beam energies of clinical interest.

Although Planskoy (1980) studied the dose rate dependence of three selected natural diamond detectors and concluded that Δ is independent of variables such as bias voltage, beam energy and modality for the tested diamonds, the conclusion was based on a composite curve plotted after averaging data for all beam energies and bias voltages used. The independence of Δ on beam energy and/or modality has also been mentioned by Laub et al. (1999), Fidanzio et al. (2004), Cirrone et al. (2006), Björk et al. (2000). On the other hand, Górka et al. (2008) observed a decreasing trend of Δ with mean photon energy and a variation of Δ with electric field has been reported by Fidanzio et al. (2004). Unlike each of the cited studies in which only one diamond detector was tested, this presentation considers a wider range of crystals. Furthermore the Δ values of the crystals were computed for different beam energies and bias voltages.

2. Experimental

Nine commercially available synthetic diamond crystals of various types and classes with sizes ranging between 5×5 and 10×10 mm^2 and thicknesses of either 0.5 or 1.0 mm were examined. The tested diamonds included eight polycrystalline chemical vapour deposition (CVD) crystals of detector grade (DG) and optical grade (OG) qualities and one high-pressure, high-temperature (HPHT) sample (Table 1). The opposite surfaces of each of the crystals were metallised as reported in a previous study (Ade et al., 2012) to provide the necessary ohmic contacts for voltage biasing and acquisition of the signal produced by ionising radiation. For quality control, identification and/or determination of defect/impurity types and levels, the crystals were characterised using Raman spectroscopy, Electron spin resonance (ESR) and Fourier transform infrared (FTIR) absorption spectroscopy. Thermoluminescence (TL) emission was also used as tool to scan the performances of the crystals.

The Raman spectra were acquired using a Jobin-Yvon T64000 Raman spectrometer with the 514.5 nm line of an Ar^+ laser as excitation source and the ESR measurements were carried out with a Bruker ESP300E ESP spectrometer in similar procedures as reported by Assiamah (2004). TL measurements were carried out under subdued light conditions (to minimise light influences on TL response) by placing each irradiated diamond crystal (using a ^{90}Sr beta source with a controlled exposure time of 30 s and delay time before readout of 15 s) into a TLD reader-model Toledo 654. The temperature was ramped up to about 350° C for luminescence–emission measurements. The integrated response from each crystal was recorded as arbitrary counts. Mid-infrared absorption spectra were recorded using a Vertex 70v IR spectrometer from Bruker, using a diamond ATR (attenuated total reflectance) cell as sample holder. The spectrometer operates in the spectral range from 4000 to 400 cm^{-1} and the instrument chamber was evacuated during spectra acquisition to eliminate interference from CO_2 and water vapour bands.

Dosimetric measurements were conducted with high-energy therapy photon (6 and 15 MV) and electron (7 and 12 MeV) beams produced by a Siemens Primus linear accelerator at the Charlotte Maxeke Johannesburg Academic Hospital. Each diamond crystal was encapsulated in a probe housing as described in a previous study (Ade et al., 2012) and the probe, placed in its customised Perspex phantom was connected to a PTW-Freiburg Unidos E electrometer system operated manually in the 'charge' mode. The probe, constructed of entirely tissue-equivalent material with a Perspex body can hold diamond crystals of various dimensions up to 10×10 mm^2 in size, has features which allow crystals to be exposed in different exposure orientations[1] ('edge-on' and 'flat-on') for impinging radiation and is furthermore compatible with commercially available electrometer systems. For each crystal, the

[1] In the 'flat-on' orientation, the incident radiation is normal to the face of the diamond wafer, which has a larger surface area but with reduced attenuation depth. In the 'edge-on' orientation (suitable for low-energy X-rays), the incident radiation is normal to a wafer edge which has a smaller area but with greater attenuation depth.

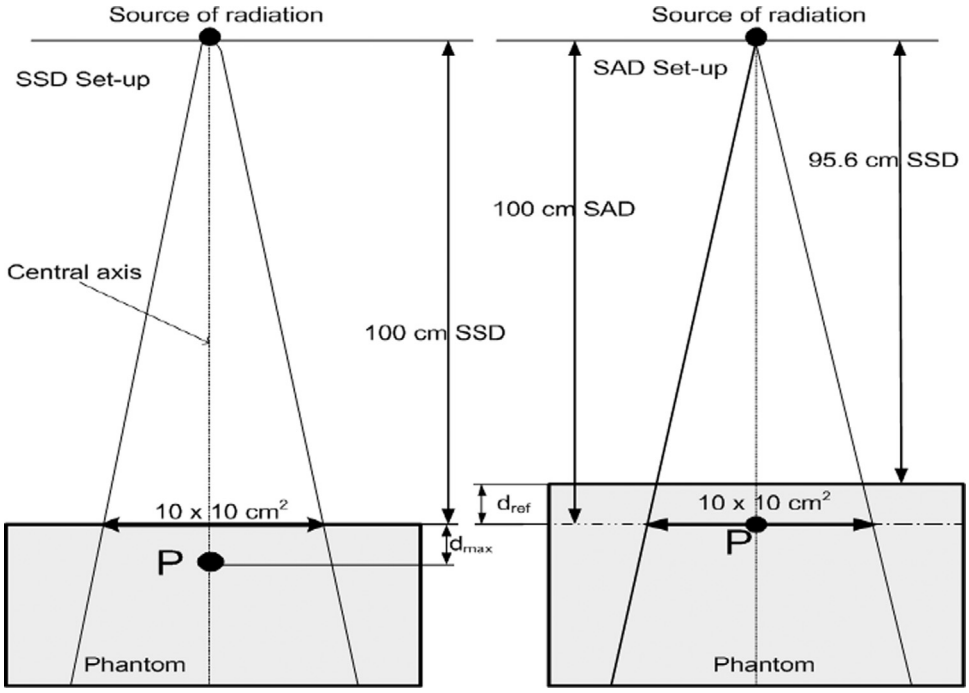

Fig. 1. Irradiation geometries for dose rate dependence measurements under reference conditions in both electron (SSD set-up) and photon (source-to-axis distance (SAD) set-up) beams. P is the effective point of measurement of the detector.

signal produced by ionising radiation was measured at +50 and +100 V bias voltages.

On exposures to the 7 and 12 MeV electron beams the dose rate dependence of each diamond detector was investigated in a similar procedure as reported in a recent study (Ade et al., 2014). For the 6 and 15 MV photon beams the diamond probe was positioned in the Perspex phantom at a reference depth (d_{ref}) of 4.4 cm (5 cm water equivalent). Variation of the dose rate was then achieved by changing the source-to-phantom surface distance (SSD) of a 10×10 cm^2 beam from 82 to 118 cm for the photon beams since dose rate is usually adjusted by varying the SSD or the pulse repetition frequency of the treatment machine (Hoban et al., 1994; Fidanzio et al., 2004). The average absorbed dose rates which varied between 1.0 and 3.07 Gy/min at each position of the probe at the depths of measurement for both beam types were measured with a 0.6 cm^3 Farmer chamber connected to Unidos E electrometer biased at +400 V. Fifty monitor units were used to irradiate each detector. The reference conditions of measurements were as follows: a dose rate of 3.0 Gy/min defined at d_{max} in phantom at 100 cm SSD with an applicator defined field of 10×10 cm^2 for the electron beams, and a dose rate of 2 Gy/min defined at d_{ref} in phantom, where d_{ref} is at the isocentre (100 cm source-to-axis distance (SAD)) of the machine and the set field size in 10×10 cm^2 for the 6 and 15 MV photon beams. The irradiation geometries for the measurements are illustrated in Fig. 1.

3. Results and discussion

3.1. Raman spectroscopy and TL response

The Raman spectra for the diamond crystals were recorded as reported in Section 2. In order to improve the statistical significance of the data, the Raman spectra for each crystal were mapped at twenty different and evenly spaced points. For each point, the data were fitted with a combined Gaussian–Lorentzian function in order to extract the Raman peak position and width. A Lorentzian profile with broadening is caused by a decrease in phonon lifetime due to scattering by lattice defects while a Gaussian profile results due to lattice strain caused by defects (Kirillov and Reynolds, 1994). For all the crystals under test, only the characteristic diamond Raman peak at ≈ 1332.8 cm^{-1} was observed over a flat background with no observable peak around 1335 and 1500 cm^{-1} which is therefore strong evidence that the crystals are pure diamonds (Prawer and Nemanich, 2004). Presented in Table 1 are the measured Raman widths (FWHM) after correction for instrumental contribution.

The residual stress S can be estimated from the frequency shift $\Delta\upsilon$ of the peak position as follows (Erasmus et al., 2011; Gracio et al., 2010; Catledge et al., 1996; Bergman and Nemanich, 1995):

$$S = (\upsilon_m - \upsilon_o)/\alpha = (\Delta\upsilon/\alpha)\ \text{GPa} \quad (2)$$

where υ_m is the measured diamond peak position, υ_o is the peak position of an unstressed diamond and α is the linear pressure coefficient (i.e. coefficient of stress-induced frequency shift). In this study a reference peak value of 1332.74 cm^{-1} for υ_o obtained for measurements conducted on a stress-free diamond sample in a similar procedure as reported by Erasmus et al. (2011) was used, unlike the other studies which assume the value of 1332 cm^{-1} for natural diamond (Gracio et al., 2010; Bergman and Nemanich, 1995). The value of α has been determined by a number of authors under truly hydrostatic conditions in diamond anvil cells and the average value (2.88 cm^{-1} GPa^{-1}) of these measurements determined by Catledge et al.(1996) is used in this study. Compressive stresses result in a shift of the diamond Raman peak to higher frequencies, and tensile stresses to lower frequencies (Erasmus et al., 2011). Displayed in Table 1 are values of the frequency shift $\Delta\upsilon$ for the diamond crystals and the corresponding residual stress values evaluated from Eq. (2). Although the residual stresses are all compressive in nature the crystals are basically stress-free as the magnitudes of the stress values are negligible within the error bars shown in the frequency shifts $\Delta\upsilon$. In comparison residual stress values of the order of 0.15–2.21 GPa have been measured in diamond thin films (Gracio et al., 2010; Bergman and Nemanich, 1995) and polycrystalline diamond tools (Erasmus et al., 2011). The stresses in the films have been attributed to the thermal mismatch

(difference in the thermal expansion coefficients) between the diamond film and its substrate (Gracio et al., 2010) as well as various impurities and defects, with sp^2-bonded carbon being the main source of residual compressive stress (Bergman and Nemanich, 1995).

The results of TL measurements (TL response, defined as TL emission per unit volume) of the investigated diamond crystals are displayed in Table 1.

3.2. ESR and FTIR absorption spectroscopy

Nitrogen (N) which is a commonly observed impurity in diamond is known to influence its radiation detection properties. It is well-known that N in diamond can occur in different forms, the dominant forms being single substitutional N (N_s) atoms (C-centre), pairs of adjacent substitutional N (A-centre or A-aggregate) and complexes of four substitutional N atoms tetrahedrally sited about a vacancy (B-centre) (Surovtsev et al., 1999). These N-related defects disturb the crystalline lattice and induce IR absorption in the one-phonon region, which is forbidden in the perfect diamond lattice (Surovtsev et al., 1999). As established by Nam et al. (1991) N_s (which is dominant in synthetic diamond) is responsible for many performance characteristics of diamond radiation detectors. Whereas ESR is a useful and non-destructive technique for the characterisation of the concentration of N_s ($[N_s]$), UV absorption can be used to identify diamonds with N complexes (Nam et al., 1991; Davies, 1999) while IR spectroscopy provides a means for the identification of aggregate N in diamond and perhaps the estimation of their concentration (Kaminsky and Khachatryan, 2001). Presented in Table 1 are values of the $[N_s]$ for the diamond crystals as determined by ESR. The reason for the much higher levels of N_s impurities of the HPHT and OG crystals compared to the DG samples has been explained in our previous study (Ade et al., 2013).

Whilst the vast majority of the N in natural diamond is found in aggregate forms where their free electrons tend to pair and no paramagnetic resonance is observed, these forms are yet to be observed unambiguously in any form of synthetic diamond (McNamara, 2003). Experimental evidence provided by McNamara (2003) however suggested that aggregate N at least in the A form may exist in some CVD diamonds. In this study the FTIR absorption spectra recorded for the diamond crystals showed distinct peaks within the spectral range of 1500–1000 cm^{-1}. However, only known peaks were identified and chosen for analysis. These included peaks occurring at 1090 (a feature characteristic of the A- and B-aggregates of N), 1282 (A-centre), 1430 (N3 nitrogen centre)[2] and 1481 (C–H centres) cm^{-1} (Zaitsev, 2001). A model for the N3 centre consists of three adjacent N atoms surrounding a vacancy whereas the C–H centres are deformational modes of sp^2-hybridised C–H bonds. Since peak areas are generally considered to be more reliable than both peak heights and FWHM as a measure of intensity, the integrated areas under the peaks were determined (Table 1) as they represent defect concentration. A software package, ORIGIN 8.0 was used for both baseline insertion and background subtraction. Only four crystals seemed to show the presence of the A-centre.

3.3. Dose rate dependence

Since detector current I is proportional to conductivity σ for parallel-plate geometry where a voltage is applied across a specimen of length and cross-sectional area (Fowler, 1966), Eq. (1) can therefore be expressed as (Laub et al., 1997; Bruzzi et al., 2000; Cirrone et al., 2006)

$$I \propto D_r^{\Delta} \quad \text{or} \quad I = I_o + RD_r^{\Delta} \tag{3}$$

where I_o expresses the contribution of leakage current to the measured detector current I and R is a fitting parameter accounting for the response of the detector. The current values determined (given by the measured charge divided by the irradiation time) as a function of dose rate with the diamond detectors were then fitted by Eq. (3) using log-to-log (or power law) plots to obtain the Δ values. The coefficient of determination r^2 of each fitted line was not less than 0.999 illustrating that the data fits the model. The Δ values determined for all the diamond sensors at 1 kV/cm ranged from 0.79–1.03 to 0.85–0.96 for the electron and photon beams, respectively. In comparison, Δ values between 0.49 and 1.16 have been reported in other studies (Planskoy, 1980; Ramkumar et al., 2001; Fidanzio et al., 2004; Laub et al., 1997, 1999; Cirrone et al., 2006; Björk et al., 2000; Hoban et al., 1994; Marczewska et al., 2007; Górka et al., 2008; Lansley et al., 2009; Tranchant et al., 2008; Betzel et al., 2010; Schirru et al., 2010; Mohamed Abdel-Rahman et al., 2012) for both natural and synthetic diamonds, and a value of 1.20 has been stated for a silicon diode (Buttar et al., 2000).

3.3.1. Influence of defect and impurity levels on the dose rate linearity index Δ

It is known that diamond detectors suitable for radiation dosimetry need a certain concentration of impurities, but that too much would (i) result to an insufficient signal being produced due to a decrease in the recombination time and (ii) cause the detector to suffer from polarisation effects (Laub et al., 1999). These two factors could cause a non-linear dose rate response (Hoban et al., 1994; Das, 2009). The results of Raman width broadening, TL response, $[N_s]$ and FTIR absorption presented in Table 1 therefore serve to provide an indication of how defect and impurity levels influence the Δ values of the diamond sensors where it is demonstrated for each class of the CVD crystals (i.e. OG or DG crystals with N_s level in ppm or ppb) that there is a tendency for Δ to decrease with increasing $[N_s]$ and increase with increasing Raman width broadening, TL emission and FTIR absorption.

Table 1 seems to indicate that for each class of the CVD diamonds the Raman width increases with increasing TL emission and FTIR absorption but decreases with an increase in $[N_s]$. While it is known that the diamond Raman-line can be shifted due to stress, the broadening of the width is known to be influenced by crystal defects or non-homogeneous distribution of stress (Pickard et al., 1998; Faggio et al., 1999; Fish et al., 1999). The results of our investigation however suggest that the broadening in the examined crystals could be largely related to defects since the crystals have negligible residual stress values as the diamond Raman peak positions are only marginally shifted with respect to that of the unstressed diamond sample. Seeing that the Raman line-width is a measure of defect concentration within the crystal, the HPHT sample having the smallest width of 2.27 cm^{-1} is the least defective crystal whereas DGA1 having the broadest width (2.60 cm^{-1}) is the most defective crystal. Similar to Raman broadening, a higher TL response implies a more defective crystal which could reflect the greater presence of trapping centres.

[2] There exists some controversy surrounding the IR absorption at 1430 m^{-1}. While its precise position varies with specimen over the range 1426–1433 cm^{-1} (Woods, 1986), Sutherland et al. (1954) considered it (1426 cm^{-1}) to be associated with the B-group (B features) lattice absorptions. This was clarified by Woods (1986) who observed that the peak near 1426 cm^{-1} increases in strength with increasing B character and that it could be directly correlated with the intensity of the platelet peak. Platelets are linear defects whose composition is also controversial (Woods, 1986) although most models suggest that N is the dominant specie. Nepsha et al. (1971) attributed the absorption peak at 1430 cm^{-1} to be due to the N3 centre which has been accepted by Zaitsev (2001) and Gaillou et al. (2010). In spite of the controversy, the evidence suggests that the defect is N related.

Although both Raman width broadening and TL emission represent defect concentration within the diamond crystals, a major drawback of Raman spectroscopy and TL is that they do not isolate defect types responsible for the broadening of the diamond Raman peak. To supplement the limitations of both techniques ESR and FTIR absorption spectroscopy were used to identify some defect/impurity types that could influence the Raman line-width. As mentioned above, Table 1 illustrates the effect of the various defect and N_s levels on the Raman line-widths. Although the relationship between N_s level and trap concentration is not yet established for CVD diamonds unlike HPHT diamonds, the observed inverse relationship between [N_s] and Raman width as illustrated in Fig. 2 could be related to the observation made by Nam et al. (1991) for HPHT diamonds that crystals with high N_s levels tend to have much lower trap concentrations than those synthesised with lower N_s levels. It can be seen that whereas the HPHT diamond has the highest N_s level of 130 ppm and lowest Raman width, DGA1 with the lowest N_s level of 3.5 ppm has the broadest Raman width. It could also be observed from each class of the CVD diamonds that crystals with high [N_s] have lower defect levels.

As demonstrated in Fig. 3, the observed correlation between [N_s] and the N-related defect levels identified by FTIR absorption could be due to the sequence of N aggregation in diamond. As discussed by Taylor et al. (1990), the sequence begins with N_s aggregating to form the more stable A-centres. Further aggregation leads to the formation of B-aggregates. Associated with B-aggregate formation is the simultaneous production of larger planar structures called platelets. A side reaction in the A→B aggregation process produces N3 centres. Platelets may eventually degrade to form a diamond with pure B character or may undergo catastrophic degradation, resulting in the formation of platelet-depleted diamonds containing mixed A- and B-centres (Woods, 1986). Therefore, as the concentration of aggregate N is increasing, that of N_s is reducing as Fig. 3 demonstrates. The feature characteristic of the A- and B-aggregates of N observed at 1090 cm^{-1} could be the platelet-depleted diamonds referred to by Woods (1986) which he termed irregular diamonds.

In addition to the influence of N_s on the defect levels of the crystals, the more defective nature of the CVD diamonds compared to the HPHT diamond could also be ascribed to their polycrystalline structure as polycrystalline materials have high defect densities due to their non-homogeneous structure (Bergonzo et al., 2007). Particularly, it is well-known that polycrystalline CVD diamonds have a large concentration of grain boundaries (Balducci et al., 2005) where electron traps are concentrated or in more defective regions (Manfredotti et al., 2006).

Although Δ increases with defect concentration, it is observed from Table 1 that DGA1 and DGA2 being crystals with very high defect levels do not have an overall better performance (Δ values show greater deviations from unity or linearity) compared to the other crystals. It is likely that a large concentration of active traps (due to the presence of a very large concentration of impurities) could be present in these crystals that could cause them to suffer from polarisation effects (Laub et al., 1999). This hypothesis is supported in the next section which treats the variation of Δ with bias voltage.

3.3.2. *Influence of bias voltage on the dose rate linearity index Δ*

Contrary to the claim made by Planskoy (1980) that Δ is independent of applied voltage, Fidanzio et al. (2004) reported that the value of Δ could approach unity at high voltages although Mohamed Abdel-Rahman et al. (2012) noted that such a variation would be at the expense of the signal-to-noise ratio (SNR) due to an increase in the leakage current as leakage currents and their fluctuations are an undesirable source of noise in radiation measurements (Kania et al., 1993). In this study the influence of bias voltage on the dose rate dependence of the diamond detectors was investigated using a 6 MV photon beam utilising two applied voltages of 50 and 100 V as presented in Table 2. The results show that Δ could vary with bias voltage. If many active traps are present within the crystals then the increase of Δ with increase in bias voltage is expected as a higher proportion of the charge carriers produced by ionising radiation would be collected at the external circuit, that is, charge collection efficiency of the detector would increase with an increase in electric field.

Although Fowler's model predicts that Δ could approach unity for a crystal with a high level of impurities (where the equilibrium density of electrons in traps is very much greater than the density of free electrons), a large trap density however results in short recombination times and therefore reduced sensitivity. In addition, due to the presence of many trapped electrons, a polarisation effect could develop which would cause a sub-linear dose rate response even at higher voltages. Evidence of trap concentration presented in this study is reflected in the results of TL response. Table 2 demonstrates that the variation of Δ with bias voltage is up to 5% for crystals with high TL response values. The greatest variation of 6.8% is shown by DGA1 which has the highest TL response. It could also be observed from Table 2 that the Δ values of DGB1, OGA and OGD decrease marginally with increase in applied voltage. Ramkumar et al. (2001) who also made a similar observation explained that it could be attributed to a reduction in the carrier life time with increase in electric field. This in turn could be

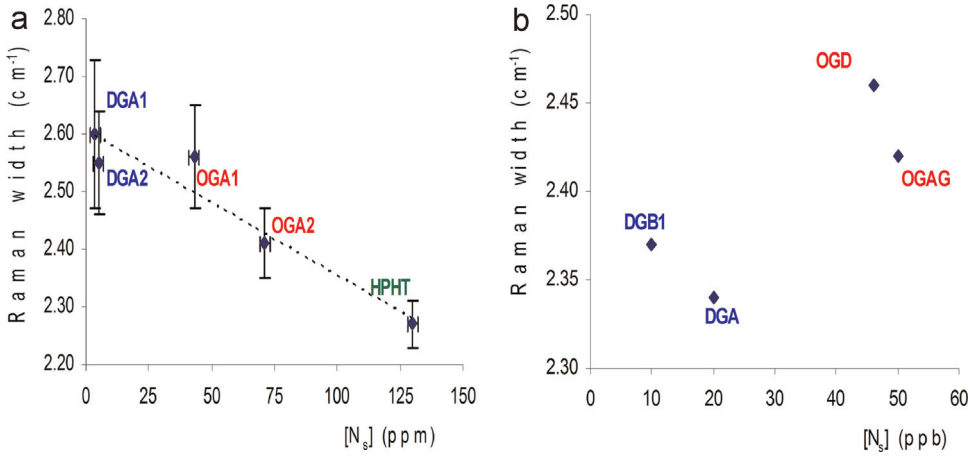

Fig. 2. Relationship between Raman width broadening and N_s level for the diamond crystals with [N_s] in (a) ppm and (b) ppb level.

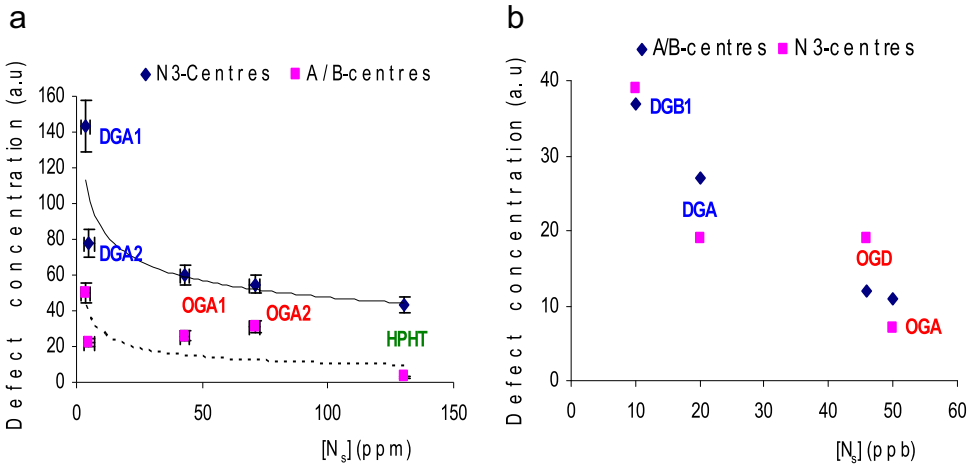

Fig. 3. Relationship between defect concentration (N-related defect levels identified by FTIR absorption) and $[N_s]$ for the diamond crystals with $[N_s]$ in (a) ppm and (b) ppb level.

a reflection of a constant carrier life time or it could be due to a polarisation effect.

Illustrated in Fig. 4(a) is the per cent change of Δ (obtained from Table 2) with TL response where it is observed that the variation increases with increasing TL response and that the change of Δ with bias voltage is within 2% when the TL response value is ≤ 2.2 arbitrary units. Plotted in Fig. 4(b) is the relationship between TL response and the sum total of the various defect levels (N3, C–H, A- and A/B-centres) presented in Table 1 as TL emission could be influenced by the combined effect of several defects. The figure demonstrates that below a concentration of ninety arbitrary units for the defect centres the TL response shows only a marginal change. Although the results suggest that the effect of the defect centres could be responsible for the trend observed in Fig. 4(a) and indicates that within a given range of these defect levels Δ would be independent of bias voltage, our investigation suggested that the N3 and C–H centres could have a dominant influence as a correlation (similar to Fig. 4(b)) between TL response and each of these two defect levels was observed unlike the 'A/B centres' where no trend was found.

3.3.3. *Dependence of Δ on beam energy and type*

Presented in Table 1 are the Δ values of the diamond detectors obtained for the two electron energies (7 and 12 MeV) and the two photon energies (6 and 15 MV). With the exception of the HPHT sample it can be observed for each beam type for the CVD diamonds that Δ seems to decrease with increasing beam energy particularly electron energy. A similar observation has also been made by Górka et al. (2008) for three different photon beam qualities for a CVD diamond detector where Δ values of 0.979, 0.937 and 0.896 were obtained for ^{60}Co γ-rays, 6 and 18 MV photons, respectively, but no reason for the observation was given. The difference in the Δ values observed between the two beam types could be attributed to the influence of defects and the different interaction cross sections of electrons and photons. The change in Δ with N_s and defect levels for each class of the CVD diamonds was considered in Section 3.3.1 and the reason for the greater deviation of the Δ values of DGA1 and DGA2 from unity compared to other crystals was attributed to a polarisation effect. Compared to HPHT diamonds charge collection efficiency in polycrystalline CVD diamonds is influenced by the presence and non-uniform distribution of defects at grain boundaries and it is known that the performance of a diamond device depends on defects both in the bulk and near the surface (Balmer et al., 2009). In this study, C–H centres have been identified as defect types possibly residing on or near the surfaces of the diamond crystals as it is well known that large concentrations of hydrogen can be found in the immediate subsurface region of a diamond crystal (Goss, 2003), unlike N-related impurities which are dominant bulk defects. Surface conduction in hydrogenated diamond has also been attributed in part to the role of subsurface hydrogen, which might take the passive form of removing dangling bonds by forming stable and inert C–H centres (Goss, 2003).

The observation made for the CVD diamonds that Δ decreases with increasing beam energy particularly electron energy could therefore be attributed to the combined influence of both surface and bulk defects (and their distribution) and the different interaction mechanisms of electrons and photons related to their penetrating power including scattered radiation. Firstly, electrons being charged particles may interact both on the surface and within the bulk (for high energy beams) of the crystals whereas photons, which are highly penetrating radiation, interaction may largely occur within the bulk of the crystals and most of the photons could pass through the crystals without any interaction. Secondly, scattering effects in the accelerator head and in the air between the exit window and phantom surface which are very pronounced for electron beams cause electrons to follow very tortuous paths, resulting in large variations of the actual path of electrons in the interacting medium compared to photons. As scattered or low-energy radiation may interact more on or near the surface of the crystals the ionisation process on the surface could be largely influenced by surface defects compared to bulk

Table 2
Influence of bias voltage on the linearity index Δ of the diamond detectors.

Δ Values (± 0.02) at	HPHT	OGA1	OGA2	DGA1	DGA2	DGA	DGB1	OGA	OGD
+50 V	0.94	0.89	0.84	0.85	0.82	0.91	0.96	0.93	0.96
+100 V	0.96	0.94	0.88	0.91	0.87	0.91	0.95	0.91	0.94
Percent (%) change	2.1	5.4	4.7	6.8	5.9	0.0	−1.0	−2.2	−2.1
TL response (a.u)	2.2	13.8	11.4	45.0	19.1	0.74	0.82	1.24	1.76

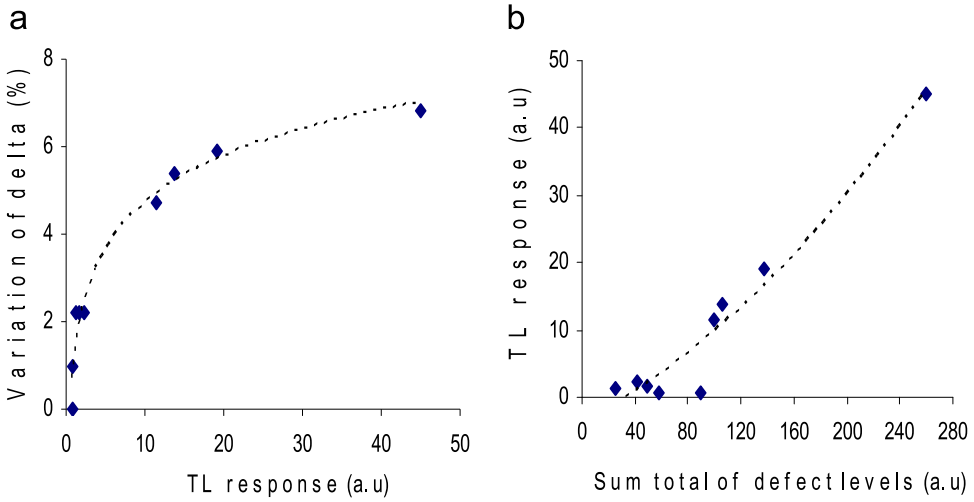

Fig. 4. (a) Percentage variation of Δ (obtained from Table 2) with TL response. (b) Variation of TL response with defect levels (sum total of N3, C–H, A- and A/B-centres).

defects which would perhaps influence ionisation within the bulk of a crystal for highly penetration radiation. Since the fraction of scattered radiation might be greater for lower-energy beam compared to a higher-energy beam, this might possibly explain why Δ decreases with increasing beam energy.

In order to quantify and evaluate the significance of the change of Δ with beam energy, the relative differences between the Δ values obtained for two different beam energies were calculated for each diamond detector. In this study, a tolerance level of $\pm 2\%$ (which coincided with the measuring accuracy) was considered for the evaluation. With this figure and considering Δ values of 1.02 and 0.98 (which give a 2% deviation from linearity) for relative dose corrections, the ICRU $\pm 5\%$ margin of absorbed dose delivery in radiotherapy (International Commission on Radiation Units and Measurements, 1976) can be achieved even when the dose rate is varied by a factor of 10 as mentioned in our recent study (Ade et al., 2014). As demonstrated in Table 3 whereas the Δ values of HPHT diamond show no dependence on the two electron and two photon energies, only those of three CVD diamonds (DGA, DGB1 and OGD with [N_s] in ppb level) show a marginal variation between the two energies of each beam type. Also whereas a very strong variation ($>5\%$) is observed between the two electron energies for three OG crystals (OGA1, OGA2 and OGA), only about a 3% variation is observed between the 6 and 15 MV photons.

Fig. 5(a) and (b) demonstrates the effects of the C–H and N3 centres, respectively on the per cent variation of Δ with beam energy (between the two energies of each beam type). Although both figures indicate that the variation of Δ between the beam energies increases with increase in both defect levels the variation is stronger for electron beams compared to photons. This observation could suggest that the electrons are more sensitive to both the C–H and N3 centres than the photons. In addition to the increasing trend observed in both Fig. 5 (a) and (b), (b) also illustrates that within a given range (between 19 and 39 arbitrary units) for the N3 defect levels, the variation of Δ between the two energies of each beam type would be within the tolerance level as clearly demonstrated in Fig. 6. Similar to the effect of the N3 and C–H defect levels on the variation of Δ with bias voltage, Figs. 5 and 6 also suggest that the combined effect of these two defect levels could have a dominant influence on the dependence of Δ on beam energy unlike the 'A/B centres' where no correlation was observed. The results of OGA1, OGA2 and OGA whose Δ values vary strongly with electron energy are omitted from Fig. 6 as they do not follow the observed trend especially the trend depicted in Fig. 5(b) in spite of the fact that these crystals have low levels of C–H centres. For the case of OGA, its N3 level is not within the range

Table 3
Dependence of the linearity index Δ on beam energy.

Specimen	Relative differences (%) between the Δ values obtained for	
	7 and 12 MeV electron beams	6 and 15 MV photon beams
HPHT	0.0	0.0
OGA1	8.9	3.2
OGA2	9.1	3.4
DGA1	4.5	2.2
DGA2	3.7	2.3
DGA	1.0	1.1
DGB1	2.0	1.0
OGA	5.1	2.2
OGD	2.0	1.1

demonstrated in Fig. 6 since the performance of the diamonds is influenced by the combined effect of the C–H and N3 levels. The poor performance of OGA1 and OGA2 might be influenced by non-uniform distribution of C–H centres as our previous study (Ade et al., 2013) indicated that the uneven distribution of defects in an OG CVD diamond have a greater influence on its performance (instability of response) compared to HPHT and DG CVD diamonds.

The small dependence of Δ ($\leq 2\%$) on beam energy observed with some of the crystals could therefore be attributed to the combined influence of defect levels within a given range and to the negligible energy dependence of diamond to radiation (this however depends on material purity and its uniformity) within a given energy range (Laub et al., 1997; van der Merwe and Keddy, 1999; Schirru et al., 2010). In particular, it is known that a low-impurity natural diamond detector shows no energy dependence to photon radiation in the energy range from 4 to 25 MV (Laub et al., 1997) and to electron radiation in the energy range from 4 to 10 MeV (Laub et al., 1999). However, using the same diamond detector a small energy dependence of about 2% is observed between 10 and 18 MeV electron beams (Laub et al., 1999). Although the energy independence of diamond to radiation is expected from theory due to the near-tissue equivalence of diamond (carbon) (Laub et al., 1999), we believe that defects (depending on type, location, concentration and distribution) could also introduce some energy dependence either by modifying its interaction cross section or introduce active traps which could influence the conductivity of the detector. In this study, 7 and 12 MeV electron, and 6 and 15 MV photon beams were considered and under the reference conditions of measurements, the change in response between the two beam energies of each radiation type was $<2\%$ for

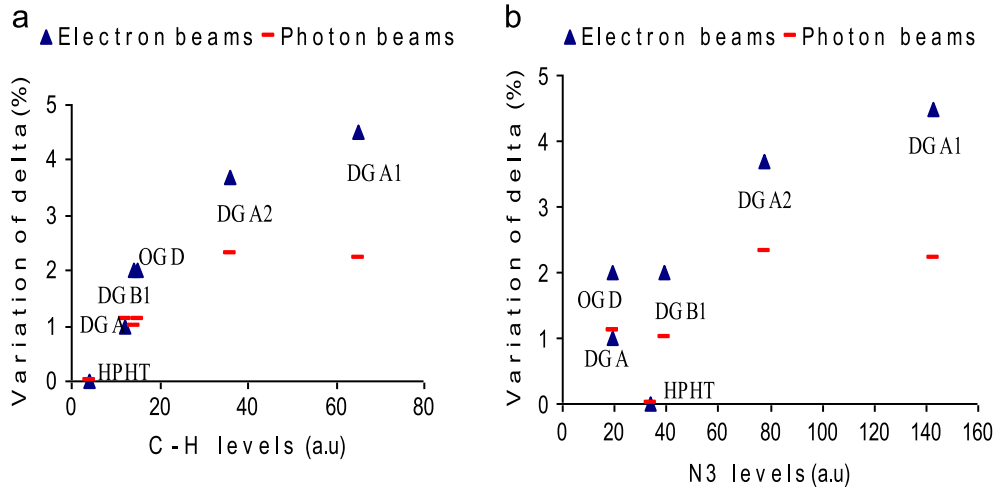

Fig. 5. Percentage variation of Δ between the two electron, and between the two photon energies (obtained from Table 3) with (a) C–H and (b) N3 centres for HPHT, DGA, DGB1 and OGD.

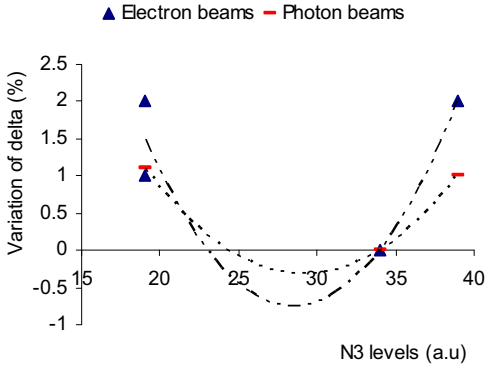

Fig. 6. The influence of N3 levels within a given range (obtained from Fig. 5 (b)) on the variation of Δ between the two electron, and between the two photon energies (for HPHT, DGA, DGB1 and OGD).

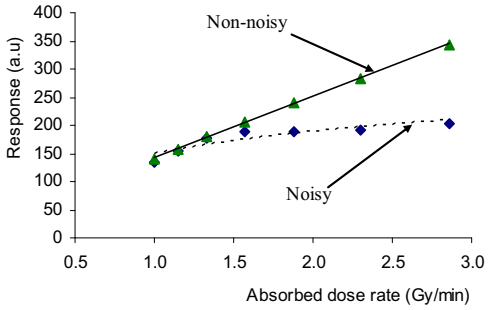

Fig. 7. The influence of background signal on the dose rate dependence of DGA1 under noisy (Δ=0.34) and non-noisy (Δ=0.85) conditions at 50 V bias.

the HPHT diamond while a variation $\geq$2% was observed for some of the CVD crystals.

While Planskoy (1980) concluded from his study that Δ is independent of applied voltage, beam energy and modality, Schirru et al. (2008) noted that Δ depends on experimental conditions such as applied electric field and Górka et al. (2008) observed an 8% difference between the Δ values obtained for three different photon beam qualities for a CVD diamond detector. In addition, a variation of Δ with applied voltage has been observed by some researchers (Ramkumar et al., 2001; Fidanzio et al., 2004; Betzel et al., 2010). The results of this study have also demonstrated that Δ could vary strongly with bias voltage, beam energy and type due to the presence and influence of defect levels. Therefore for a given diamond detector especially the polycrystalline CVD diamonds Δ should be investigated for every beam type at a given bias voltage for clinical use.

3.3.4. *The influence of leakage current on the dose rate response*

It is well-known that leakage (dark) current and its fluctuations are an undesirable noise source in radiation measurements and can limit the magnitude of the applied electric field (Kania et al., 1993), and that the sensitivity of a diamond detector to radiation depends on the ionisation signal-to-dark current ratio (Manfredotti et al., 1998). Dark current is the relatively small electric current that flows through a device in the absence of irradiation, and its magnitude could be influenced by a number of factors including contact material. Therefore an important factor to consider in the dosimetric characterisation of a solid-state detector such as a diamond detector with its relatively high impedance is minimisation and stabilisation of the background signal or dark current since its effect may obscure the magnitude of the measured signal.

From the above discussion, the parameter I_o (Eq. (3)) which expresses the contribution of the leakage current to the measured detector current I, might therefore influence the dose rate dependence of a given detector depending on its magnitude and fluctuation. In this study the leakage current of each diamond detector which was observed to be greatly influenced by ambient light was investigated in a similar procedure as reported in a previous study (Ade et al., 2012). The HPHT sample was found to have the lowest dark current value which did not vary between irradiations compared to its CVD counterparts and it was observed that the dark current increases with applied voltage. Presented in Table 1 are the dark current values of the diamond crystals at 1 kV/cm when the diamond probe was connected to the Unidos E electrometer system using a detector cable of about 10 m in length.

The determination of the Δ values presented in Table 1 took into account the contribution of the leakage currents. However, to investigate the influence of leakage current on the dose rate response, DGA1 with the highest value of dark current was exposed to ambient light. Under this condition the background signal increases and fluctuates randomly, thus influencing measurements. The response of the detector under noisy (exposed to light)[3] and non-noisy (shielded from light) conditions at 50 V bias is plotted in Fig. 7 as a function of dose rate. The Δ values computed under the noisy

[3] In this study, noisy conditions refer to the presence of ambient light of intensity $\leq$1912 lx measured with a lux metre (Model 91150V, Oriel Instruments).

and non-noisy conditions were 0.34 and 0.85, respectively. These results illustrate that under the noisy conditions the detector shows a very strong dose rate dependence suggesting therefore that extra care should be exercised when performing dosimetric measurements in a noisy environment.

4. Conclusions

In this study, the influence of defect levels, bias voltage, leakage current, beam energy and type on the dose rate dependence of nine synthetic diamond detectors of various types was investigated in the dosimetry of high-energy photon (6 and 15 MV) and electron (7 and 12 MeV) therapy beams. The linearity index Δ was determined for each diamond detector and evaluated for its dependence on bias voltage, beam energy and type. The results highlighted the importance of using more than one beam energy from each radiation type to probe the performances of the crystals. The results demonstrated that within an accuracy of 2% only the Δ values of the HPHT diamond detector were independent of both beam energy and type, whereas only those of DGA, DGB1 and OGD were independent of the two beam energies of each radiation type. However, within the limits of experimental uncertainty only the Δ values of OGA1 and OGA2 showed a marginal dependence on the photon beams compared to the electron beams. The independence of Δ on beam energy and type as observed with the HPHT diamond is advantageous in clinical dosimetry as Δ could be determined only once for any given beam energy and then used for other energies of clinical interest. The Δ values of the diamonds were found to change with various defect levels and it was observed that the Δ values of crystals with high defect levels varied with bias voltage. Furthermore differences in crystal quality due to the presence of defect levels could cause Δ to show a variation with bias voltage, beam energy and type. The influence of the defect levels on the sensitivity values of the crystals is under investigation.

Acknowledgements

This on-going project is funded by the Department of Science and Technology, Republic of South Africa and National Research Foundation (DST-NRF Centre of Excellence in Strong Materials, Grant No. 41292). Prof. J. van Wyk and Dr. R. Erasmus are acknowledged for ESR and Raman spectroscopy measurements, respectively. The authors would also like to thank Prof. Debbie van der Merwe for useful and valuable discussions.

References

Ade, N., Nam, T.L., Assiamah, M., 2012. Radiat. Phys. Chem. 81, 232.
Ade, N., Nam, T.L., Mhlanga, S.H., 2013. Radiat. Phys. Chem. 86, 42.
Ade, N., Nam, T.L., Derry, T.E., Mhlanga, S.H., 2014. Radiat. Phys. Chem. 98, 155.
Assiamah, M., 2004. PhD thesis. University of the Witwatersrand, Johannesburg.
Balducci, A., Marinelli, Macro, Milani, E., Morgada, M.E., Prestopino, G., Scoccia, M., Tucciarone, A., Verona-Rinati, G., 2005. Appl. Phys. Lett. 87, 222101.
Balmer, R.S., Brandon, J.R., Clewes, S.L., Dhillon, H.K., Dodson, J.M., Friel, I., Inglis, P.N., Madgwick, T.D., Markham, M.L., Mollart, T.P., Perkins, N., Scarsbrrok, G.A., Twitchen, D.J., Whitehead, A.J., Wilman, J.J., Woollard, S.M., 2009. J. Phys.: Condens. Matter 21, 364221.
Bergman, L., Nemanich, R.J., 1995. J. Appl. Phys. 78, 6709.
Bergonzo, P., Tromson, D., Descamps, C., Hamrita, H., Mer, C., Tranchant, N., Nesladek, M., 2007. Diam. Relat. Mater. 16, 1038.
Betzel, G.T., Lansley, S.P., Baluti, F., Reinisch, L., Meyer, J., 2010. Nucl. Instrum. Methods Phys. Res. A 614, 130.
Björk, P., Knöös, T., Nilsson, P., 2000. Med. Phys. 27, 2580.
Bruzzi, M., Bucciolini, M., Cirrone, G.A.P., Cuttone, G., Mazzocchi, S., Pirollo, S., Sciortino, S., 2000. Nucl. Instrum. Methods Phys. Res. A 454, 142.
Buttar, C.M., Airey, R., Conway, J., Hill, G., Ramkumar, S., Scarsbrook, G., Sussmann, R.S., Walker, S., Whitehead, A., 2000. Diam. Relat. Mater. 9, 965.
Catledge, S.A., Vohra, Y.K., Ladi, R., Rai, G., 1996. Diam. Relat. Mater. 5, 1159.
Cirrone, G.A.P., Cuttone, G., Lo Nigro, S., Mongelli, V., Raffaele, L., Sabini, M.G., 2006. Nucl. Phys. B (Proc. Suppl.) 150, 330.
Das, I.J., 2009. Diamond detector. In: Rogers, D.W.O., Cyglar, J.E. (Eds.), Clinical Dosimetry Measurements in Radiotherapy. Medical Physics Publishing, Madison, WI, pp. 891–912.
Davies, G., 1999. Physica B 273, 15.
Erasmus, R.M., Comins, J.D., Mofokeng, V., Martin, Z., 2011. Diam. Relat. Mater. 20, 907.
Faggio, G., Marinelli, M., Messina, G., Milani, E., Paoletti, A., Santangelo, S., Verona-Rinati, G., 1999. Microsyst. Technol. 6, 23.
Fidanzio, A., Azario, L., Viola, P., Ascarelli, P., Capelli, E., Conte, G., Piermattei, A., 2004. Nucl. Instrum. Methods Phys. Res. A 524, 115.
Fish, M.L., Massler, O., Reid, J.A., MacGregor, R., Comins, J.D., 1999. Diam. Relat. Mater. 8, 1511.
Fowler, J.F., 1966. Solid State Electrical Conductivity Dosimeters. Radiation Dosimetry, vol. II. AcademicNew York p. 291.
Gaillou, E., Post, J.E., Bassim, N.D., Zaitsev, A.M., Rose, T., Fries, M.D., Stroud, R.M., Steele, A., Butler, J.E., 2010. Diam. Relat. Mater. 19, 1207.
Górka, B., Fernandez-Varea, J.M., Panettieri, V., Nilsson, B., 2008. Nucl. Instrum. Methods Phys. Res. A 593, 578.
Goss, J.P., 2003. J. Phys.: Condens. Matter 15, R551.
Gracio, J.J., Fan, Q.H., Madaleno, J.C., 2010. J. Phys. D: Appl. Phys. 43, 374017.
Hoban, P.W., Heydarian, M., Beckham, W.A., Beddoe, A.H., 1994. Phys. Med. Biol. 39, 1219.
International Commission on Radiation Units and Measurements, 1976. Determination of Absorbed Dose in a Patient Irradiated by Beams of X or Gamma Rays in Radiotherapy Procedures, ICRU Report 24. ICRU, Bethesda.
Kaminsky, F.V., Khachatryan, G.K., 2001. Can. Mineral. 39, 1733.
Kania, D.R., Landstrass, M.I., Plano, M.A., 1993. Diam. Relat. Mater. 2, 1012.
Kirillov, D., Reynolds, G.J., 1994. Appl. Phys. Lett. 65, 1641.
Lansley, S.P., Betzel, G.T., Meyer, J., Baluti, F., Reinisch, L., Meyer, J., 2009. Nucl. Instrum. Methods Phys. Res. A 607, 659.
Laub, W.U., Kaulich, T.W., Nusslin, F., 1997. Phys. Med. Biol. 24, 535.
Laub, W.U., Kaulich, T.W., Nusslin, F., 1999. Phys. Med. Biol. 44, 2183.
Manfredotti, C., Apostolo, G., Fizzotti, F., LoGiudice, A., Morando, M., Pignolo, R., Polesselo, P., Truccato, M., Vittone, E., Nastasi, U., 1998. CVD diamond tips as X-ray detectors. Diam. Relat. Mater. 7, 523.
Manfredotti, C., Fizzotti, F., Garino, Y., 2006. Diam. Relat. Mater. 15, 1362.
Marczewska, B., Kupriyanov, I., Pal'Yanov, Yu, Nowak, T., Olko, P., Rębisz, M., Waligórski, M.P.R., 2007. Diam. Relat. Mater. 16, 191.
McNamara, K.M., 2003. Appl. Phys. Lett. 83, 1325.
Mohamed Abdel-Rahman, A.E., Lohstroh, A., Jayawardena, I., Henley, S.J., 2012. Diam. Relat. Mater. 22, 70.
Nam, T.L., Karfunkel, U., Keddy, R.J., Every, A.G., 1991. Radiat. Eff. Defects Solids 116, 233.
Nepsha, V.I., Zvonkov, S.D., Dudenkov, Yu, A., Klyuev, Yu, A., Zubkov, V.M., 1971. Diamonds 2, 1.
Pickard, C.D.O., Davis, T.J., Wang, W.N., Steeds, J.W., 1998. Diam. Relat. Mater. 7, 238.
Planskoy, B., 1980. Phys. Med. Biol. 25, 519.
Prawer, S., Nemanich, R., 2004. Philos. Trans. R Soc. Lond. A 362, 2537.
Ramkumar, S., Buttar, C.M., Conway, J., Whitehead, A.J., Sussman, R.S., Hill, G., Walker, S., 2001. Nucl. Instrum. Methods Phys. Res. A 460, 401.
Schirru, F., Kupriyanov, I., Marczewska, B., Nowak, T., 2008. Phys. Status Solidi A 205, 2216.
Schirru, F., Kisielewicz, K., Nowak, T., Marczewska, B., 2010. J. Phys. D: Appl. Phys. 43, 265101.
Surovtsev, N.V., Kupriyanov, I.N., Malinovsky, V.K., Gusev, V.A., Pal'yanov, Yu, N., 1999. J. Phys.: Condens. Matter 11, 4767.
Sutherland, G.B.B.M., Blackwell, D.E., Simeral, W.G., 1954. Nature 174, 901.
Taylor, W.R., Jacques, A.L., Ridd, M., 1990. Am. Mineral. 75, 1290.
Tranchant, N., Tromson, D., Descamps, C., Isambert, A., Hamrita, H., Bergonzo, P., Nesladek, M., 2008. Diam. Relat. Mater. 17, 1297.
van der Merwe, D.G., Keddy, R.J., 1999. Radiat. Phys. Chem. 54, 325.
Woods, G.S., 1986. Proc. R Soc. Lond. A 407, 219–238.
Zaitsev, A.M., 2001. Optical Properties of Diamond. Springer Edition, Germany.